The Impact of North Atlantic Wind and Cyclone Trends on European Precipitation and Significant Wave Height in the Atlantic

Ricardo M. Trigo,[a,b] Maria A. Valente,[a,c] Isabel F. Trigo,[a,d] Pedro M. A. Miranda,[a] Alexandre M. Ramos,[a] Daniel Paredes,[e] and Ricardo García-Herrera[e]

[a]*Centro de Geofísica da Universidade de Lisboa, Faculdade de Ciências, Lisbon, Portugal*

[b]*Departamento de Engenharias, Universidade Lusófona, Lisbon, Portugal*

[c]*Instituto Geofísico do Infante Dom Luiz, Universidade de Lisboa, Lisbon, Portugal*

[d]*Instituto de Meteorologia, Lisbon, Portugal*

[e]*Departamento Física de la Tierra II, Facultad de Físicas, Universidad Complutense de Madrid, Madrid, Spain*

An analysis of the frequency of cyclones and surface wind velocity for the Euro–Atlantic sector is performed by means of an objective methodology. Monthly and seasonal trends of cyclones and wind speed magnitude are computed and trends between 1960 and 2000 evaluated. Results reveal a significant frequency decrease (increase) in the western Mediterranean (Greenland and Scandinavia), particularly in December, February, and March. Seasonal and monthly analysis of wind magnitude trends shows similar spatial patterns. We show that these changes in the frequency of low-pressure centers and the associated wind patterns are partially responsible for trends in the significant height of waves. Throughout the extended winter months (October–March), regions with positive (negative) wind magnitude trends, of up to 5 cm/s/year, often correspond to regions of positive (negative) significant wave height trends. The cyclone and wind speed trends computed for January–March are well matched by the corresponding trends in significant wave height, with February being the month with the highest trends (negative south of lat 50°N up to −3 cm/year, and positive up to 5 cm/year just north of Scotland). Trends in European precipitation are assessed using the Climatic Research Unit data set. The results of the assessment emphasize the link with the corresponding tendencies of cyclone frequencies. Finally, it is shown that these changes are associated, to a large extent, with the preferred phases of major large-scale atmospheric circulation modes, particularly with the North Atlantic Oscillation, the eastern Atlantic pattern, and the Scandinavian pattern.

Key words: **storm tracks; wind; significant wave height; precipitation; trends; NAO; EA; SCAND**

Introduction

Observational studies indicate significant climate trends at different time scales over the entire North Atlantic basin and associated large climatic changes in the two adjacent continents North America and Europe.[1] The analysis for the entire 20th century reveals positive trends in temperature for both land masses and also over the majority of the Atlantic Ocean area, with the exception of the area south of Greenland (which was characterized by a cooling trend). However, if one restricts the analysis to the last three decades, the positive trend is steeper and affects the entire North Atlantic

Ocean and European continent, in every season of the year, particularly over Europe.[2] Concerning precipitation, the last century was characterized by a positive trend for the eastern half of the North American continent and northern Europe.[1] Southern Europe (Mediterranean basin), however, suffered a slight decrease in rainfall.[3,4] In recent decades, the asymmetrical trends of precipitation in Europe have been enhanced, i.e., northern (southern) Europe is under a positive (negative) precipitation trend.[5] Spatial patterns of precipitation trends are more difficult to characterize than those obtained for temperature trends, as the precipitation regime can vary considerably over relatively short distances. Moreover, precipitation trends can present significant discrepancies within each season that can easily undermine any trend analysis performed at the seasonal scale.[6] For example, in recent decades a significant decrease (increase) in spring precipitation in southwestern (northwestern) Europe has been detected and described.[5,7–9] However, it has now been shown that such trends are mostly concentrated in the month of March, particularly the outstanding decline of March precipitation throughout the western Mediterranean sector, which does not occur in April and May.[10]

Linear trends of Significant Wave Height (SWH) for the period 1950 to 2002 have been shown to be statistically significant and positive over most of the mid-latitudinal North Atlantic.[11] These results have been confirmed with hindcasts of waves for the Atlantic Ocean that have shown an increase in mean SWH and also an increase in SWH extremes during the last four decades.[12–14] Naturally these changes in SWH are linked to changes to the two main sources of SWH, namely a) the local surface wind speed and b) the swell component that is largely determined by the frequency and intensity of remote storms.[1]

The physical processes responsible for these trends and changes seem to be acting on a hemispheric to global scale, including external forcings and changes in large-scale atmospheric circulation, with a negligible role being played by local and regional factors, such as changes in land use. It is now widely accepted that changes in atmospheric circulation imply significant changes in: wind patterns, favored storm track routes, precipitation patterns, oceanic wind-driven waves, and surface fluxes.[1,15] In particular, several studies have shown that cyclone activity over the northern Atlantic has changed throughout the second half of the 20th century with a poleward shift in storm track location and increased storm intensity, but a decrease in total storm numbers, e.g., Refs. 16, 17. The magnitude and spatial pattern of trends in cyclone activity are sensitive to the storm tracking methodology as well as to the reanalysis data set used.[18]

Station pressure data over the North Atlantic–European sector (NAE, defined between lat 25–70°N and long 75°W–20°E) shows a decline in storminess from high levels between the late 19th century to lower levels during the 1960s, followed by an increase to maximum levels around 1990 and dropping slightly subsequently.[19–21] Recent results from studies of the long-term variability of storminess affecting the Azores archipelago have corroborated this picture, although the minimum activity was found during the 1950s.[22,23] On the other hand, several studies have provided evidence for a similar temporal evolution of surface wind extremes over western Europe where the late 1980s and 1990s were characterized by more frequent storms and high wind speeds,[19,24,25] which were responsible for high losses of insured property.[23,26] We intend to assess trends of cyclonic activity based on the objective methodology developed by one of us to detect and track all mid- and high-latitude Atlantic (and Mediterranean) cyclones.[5,27,28] This approach enables the evaluation of interannual variability and trends of cyclone frequencies for the NAE region and relates these with continental climate trends and changes of ocean wave height.

It is now widely accepted that most large-scale modes of atmospheric circulation in the Northern Hemisphere have already been

described in the existing literature.[29,30] It should be stressed that the relevance of these modes is seasonally dependent, i.e., they only have a signature during part of the year.[29] Different approaches have been developed over the last decade to assess the impact of the most relevant modes on the European climate, mostly in terms of precipitation and temperature fields. Generally speaking, these studies can be clustered within two different approaches[31]:

a) Studies based on atmospheric circulation indices independently from surface climate parameters. These include the pioneering work on blocking episodes by Refs. 32–34 and, more recently, on the North Atlantic Oscillation (NAO) pattern.[35,36] At shorter spatio–temporal scales, there are various regional classification schemes, such as the Lamb Weather Types for the U.K.[37,38] and the Grosswetterlagen catalogs[39] for central Europe.
b) Methods that incorporate both atmospheric circulation and surface climatic fields, often based on eigenvalue techniques (e.g., canonical correlation analysis and singular value decomposition). Some of these works have focused on the link between atmospheric circulation over the NAE area and the climate of Europe, e.g., Refs. 4, 40–42.

Despite their different methodologies, these studies tend to agree that the most important modes of atmospheric circulation at the monthly/seasonal timescale are: a) the NAO, b) the eastern Atlantic (EA) pattern, sometimes identified as the eastern Atlantic/Western Russia pattern (EA/WR; EU2 of Ref. 29), and c) the Scandinavian pattern (SCAND; EU1 of Ref. 29). We will focus our analysis on the impact of the modes that most significantly affect the climate of Europe and Atlantic wave height, and these are: NAO, EA, and SCAND. While these modes are defined throughout the year, their strength varies considerably, being more prominent in winter and less well defined in the summer months.[29,40,43] Moreover, the impact of these major circulation modes upon the precipitation of Europe is also greater during the winter months.[41,43] Therefore, our analysis will be restricted to the extended winter season that spans between October and March.

The main objectives of this paper are twofold and can be summarized as follows:

a) to analyze monthly trends in cyclone activity and wind speed and relate such changes with the corresponding trends in European precipitation and SWH over the North Atlantic basin;
b) to evaluate the link between the interannual variability of these variables and major large-scale circulation modes, namely the NAO, the EA pattern, and the SCAND pattern.

Data Sets and Methodology

European Precipitation

Monthly values of precipitation between 1960 and 2000 for the entire European continent and part of North Africa were obtained from the high resolution (0.5° latitude by 0.5° longitude) data set developed by New *et al.*[44,45] at the Climatic Research Unit (CRU). This data set uses a dense network of observations, particularly over Europe. The spatial patterns of monthly average precipitation over Europe can be seen in Figure 1.

Storm Tracks and Wind

The analysis of atmospheric circulation at the monthly and synoptic scales over the NAE sector (lat 20–75°N, long 85°W–70°E) was based on the European Centre for Medium-Range Weather Forecasts (ECMWF) reanalysis (ERA-40) data set from 1960 until 2000.[46] Geopotential height at 1000 hPa, wind components (zonal (u) and meridional (v)), and sea level pressure (SLP) fields have been extracted from the $1.125° \times 1.125°$ regular grid. The
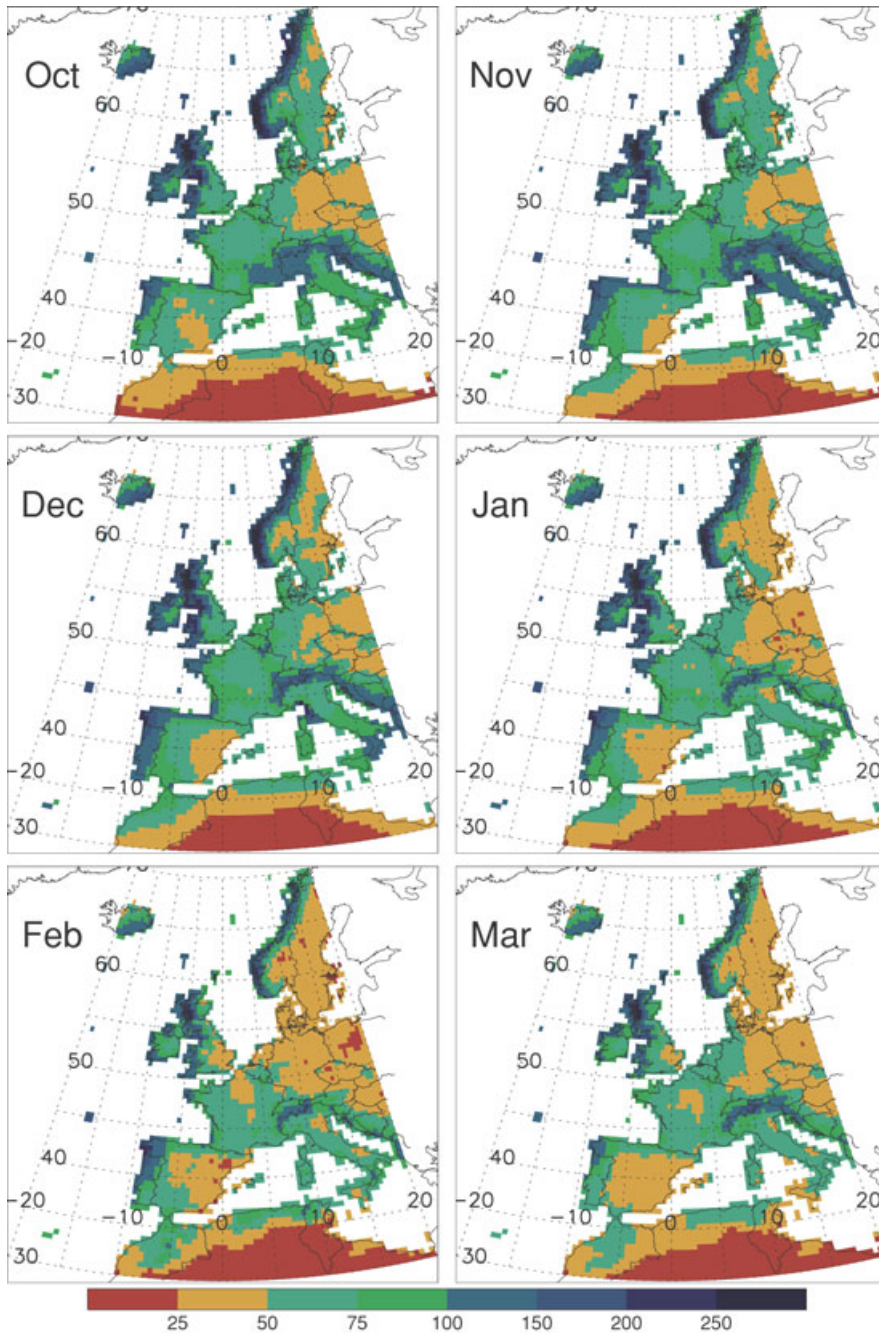
Figure 1. Monthly averages of precipitation (mm/month) for individual winter months, computed for the period 1960–2000.

average extended winter (October–March) wind speed pattern can be appreciated in Figure 2. Monthly and seasonal trends for the *u* and *v* components and 10-m wind speed were also computed.

A number of distinct objective methodologies have been developed to track paths of individual storms.[16,47–51] These different approaches and the availability of several reanalysis comprehensive data sets
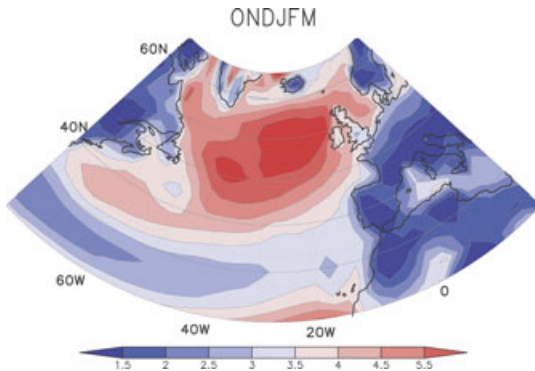
Figure 2. Seasonal average of 10-m wind speed (m/s) obtained for the extended winter (October–March) for the period 1960–2000.

have enabled the compilation of long-term climatologies.[5,17,24,52,53] Several approaches have compared cyclonic tracking methods as well as original data set resolution.[5,18,54,55] Here, the detection and tracking of North Atlantic cyclones is based on the algorithm first developed for the Mediterranean region by Trigo *et al.*[28,51] and recently adapted to the entire North Atlantic area.[5,56] For storm-tracking purposes we have used the reanalysis full spatial resolution $1.125° \times 1.125°$ grid for the entire NAE sector. Cyclones are identified as minima in geopotential height fields at 1000 hPa, fulfilling a set of conditions regarding the central pressure and the geopotential gradient. The tracking is based on a nearest neighbor search in consecutive charts, assuming that the speed of individual storms is less than 50 km/h in the westward direction and 110 km/h in any other. Further details on the cyclone-detecting and tracking methodology may be found in Trigo *et al.*[28,51] and Trigo.[5] For the purpose of this study, only lows lasting a minimum of 24 h and presenting minimum pressure values below 1010 hPa throughout their life cycle were considered.

As an example, we show in Figure 3 the complete trajectories of every cyclone with a minimum life span of 3 days detected during February 2000 in the NAE. The dots within individual storm tracks correspond to the cyclone centers that were detected on 6-h SLP

fields. It is important to keep in mind that this type of algorithm identifies and follows cyclone centers. Therefore, the cyclone's associated impact on precipitation extends to the south of each path, accompanying the main fronts associated with the synoptic systems tracked by the algorithm.[57]

Long-term averages of cyclone counts were computed at both monthly and seasonal scales for the period 1960–2000, and the individual winter monthly averages between October and March can be observed in Figure 4. EA monthly averages of cyclone counts are associated with the corresponding monthly precipitation observed over the European continent (Fig. 1).

Significant Wave Height

The monthly SWH presented here was obtained from the ERA-40 reanalysis through the Koninklijk Nederlands Meteorologisch Instituut (KNMI). These data, obtained initially from the original 6-h global fields, were used to elaborate the KNMI ERA-40 wave atlas available at http://www.knmi.nl/waveatlas.[13,58] The horizontal resolution of the global fields used here is $1.5° \times 1.5°$. The ERA-40 reanalysis used a coupled atmosphere–wave model [Integrated Forecasting System (IFS)] with variational data assimilation.[59] IFS is a state-of-the-art model, very similar to the one used operationally by ECMWF for weather forecasts, though with lower resolution. The wave model used in IFS is WAM,[60] a third-generation model in which the wave spectrum is computed by integration of the energy balance equation without any prior restriction of the spectral shape.[13] From the full spectrum, integral quantities, such as SWH or mean wave frequency, are calculated.

The SWH is equivalent to the average of the highest one-third of waves in a sea state, corresponding to what an experienced sailor would report to characterize the wave height. The SWH is computed as four times the square-root of the 0-order spectral moment, with the
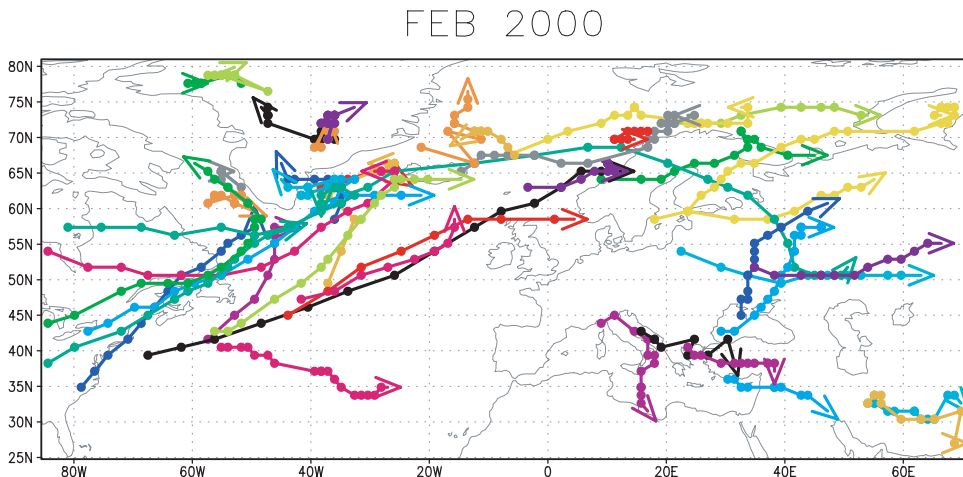
Figure 3. Path of individual cyclones detected by applying the storm-track methodology developed by Trigo[5] for the month of February 2000. Dots within individual storm tracks correspond to the cyclone centers that were detected on 6-h sea level pressure fields. Only cyclones lasting at least 3 days are depicted.

directional wave spectra being calculated by the ERA-40 wave model. According to Ref. 13, among the caveats of the ERA-40 SWH data presented in the KNMI wave atlas is the fact that the estimates are based on data averaged on a $1.5° \times 1.5°$ area and time averaged on 6 h. The approximate time a long wave would take to cross the diagonal of such a grid cell at mid-latitude is about 3 h. Therefore, for short time or space scales, waves can be higher than those represented in ERA-40. Moreover, tropical storms are not properly resolved on a $1.5° \times 1.5°$ grid. In regions of tropical cyclones, extreme wave heights are, therefore, expected to be higher than in the ERA-40 data set. It should be noted also that the ERA-40 model does not account for shallow water effects and, therefore, the ERA-40 ocean wave data is only valid in deep water regions.

The SWH data was subjected to a validating procedure using buoy observations and altimeter measurements. This validation process encountered deficiencies in the ERA-40 SWH data set. The problems found with the ERA-40 SWH data are the existence of heterogeneities in time, which limits the use of the data for studies of climate variability and trends, and the underestimation of high wave heights.[13] The data was corrected by KNMI through a non-parametric method that predicts the bias between SWH ERA-40 data and TOPEX altimeter measurements,[58] and the corrected new global 6-h data set C-ERA-40 was the end result. Comparison of the C-ERA-40 data set with SWH measurements from buoy observations and global altimeter data shows clear improvements in both biases, scatter and quantiles in the whole range of SWH values, as well as the removal of the heterogenities that were caused by changes in altimeter wave height assimilation.[13] The KNMI has supplied a 31-year subset of the ERA-40 and C-ERA-40 data for the period 1970–2000. The 1970–2000 climatology of the extended winter SWH in the NAE region is presented in Figure 5 for the original (left) and corrected (right) data. Corrected ERA-40 values are higher than non-corrected ones. Maximum values, which are located south of Greenland and Iceland at the British Isles' latitude, are just above 4 m in the original data and are just below 5 m in the C-ERA-40 data set. The Mediterranean Sea has wave heights below 2 m during the 6-month cold season.

Large-scale Circulation Patterns

Different approaches have been developed to derive the main atmospheric circulation
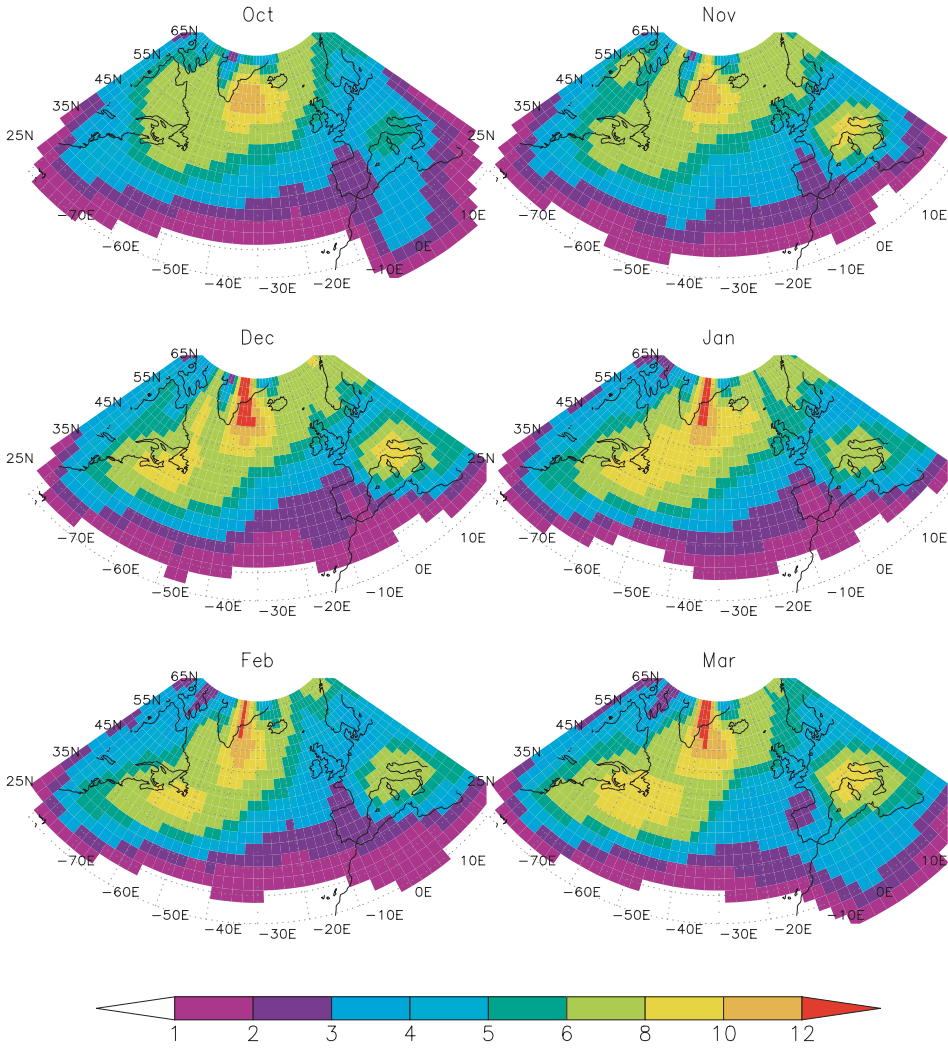
Figure 4. Monthly averages of cyclone counts for individual winter months. Statistics were computed for cell boxes with 9° longitude by 9° latitude for the period 1960–2000.
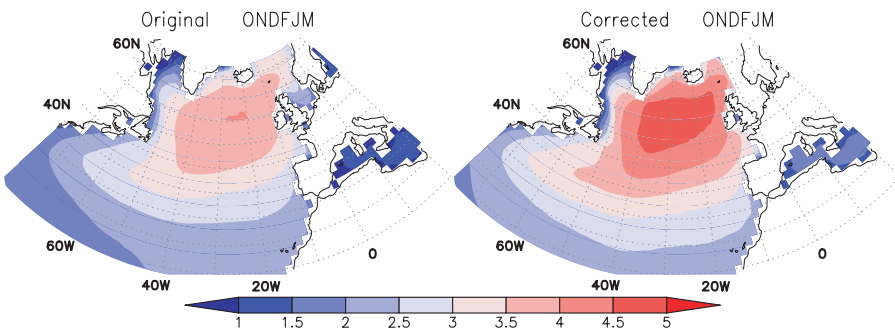

Figure 5. Mean significant wave height (m) for the 6 months October–March (1970–2000) (left, original ERA-40 values; right, corrected ERA-40 values).

patterns (also referred to as teleconnections) that characterize large-scale circulation over the entire Northern Hemisphere[29,30] as well as their impact on European climate, e.g., Refs. 61–63. Readers interested in a comprehensive description of the different methodologies to obtain these patterns and their associated impact in European climate can refer to Refs. 36 and 64. Here, the teleconnection indices were obtained from the Climate Prediction Center (CPC) from the National Oceanic and Atmospheric Administration (NOAA) (http://www.cpc.noaa.gov/data/teledoc/nao.shtml) for the period that spans between 1960 and 2000. The methodology employed by CPC to identify the Northern Hemisphere teleconnection patterns is based on rotated principal component analysis[29] applied to monthly mean standardized 500-mb geopotential height anomalies. Spatial patterns of the three main teleconnections over the NAE region can be seen in Figure 6 and represent the NAO (top), EA (middle), and SCAND (bottom) patterns. This figure represents the temporal correlation between the monthly standardized height anomalies at each point and the monthly teleconnection pattern time series from 1960 to 2000.

Figure 6. Spatial patterns of teleconnection indices North Atlantic Oscillation (NAO), eastern Atlantic (EA), and Scandinavia (SCAND) computed for December–February within the period 1960–2000.

Trend Analysis

Wind and Cyclone Trends

Long-term decadal trends of cyclone densities were computed at both monthly and seasonal scales for the period 1960–2000. Graphics were computed on cell boxes with 9° longitude by 9° latitude for the period 1960–2000. Results obtained for the individual extended winter months can be seen in Figure 7 and are shown only for cells with the most pronounced trends (>5% per decade). Furthermore, results are restricted to grid boxes with at least 1 cyclone count on average for the whole study period, which eliminates a larg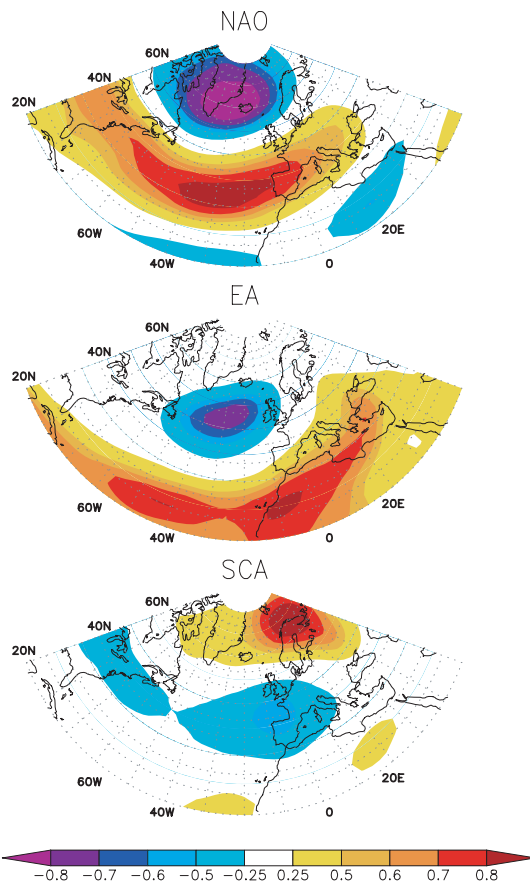e section of the subtropical Atlantic. The corresponding trends of near surface wind speed are represented in Figure 8. The two figures appear to be generally in good agreement, showing consistent trends for both variables. In particular, the Iberian Peninsula and the Mediterranean basin show a decline of both cyclonic activity and wind speed throughout the entire extended winter period. Looking at these two figures, it is possible to distinguish a different behavior for each winter half. The months between October and December are generally characterized by an increase in wind speed and some cyclonic activity in several sectors of the Northern Atlantic basin. The second part of winter, between January and March, presents a very distinct pattern with different trend signals being
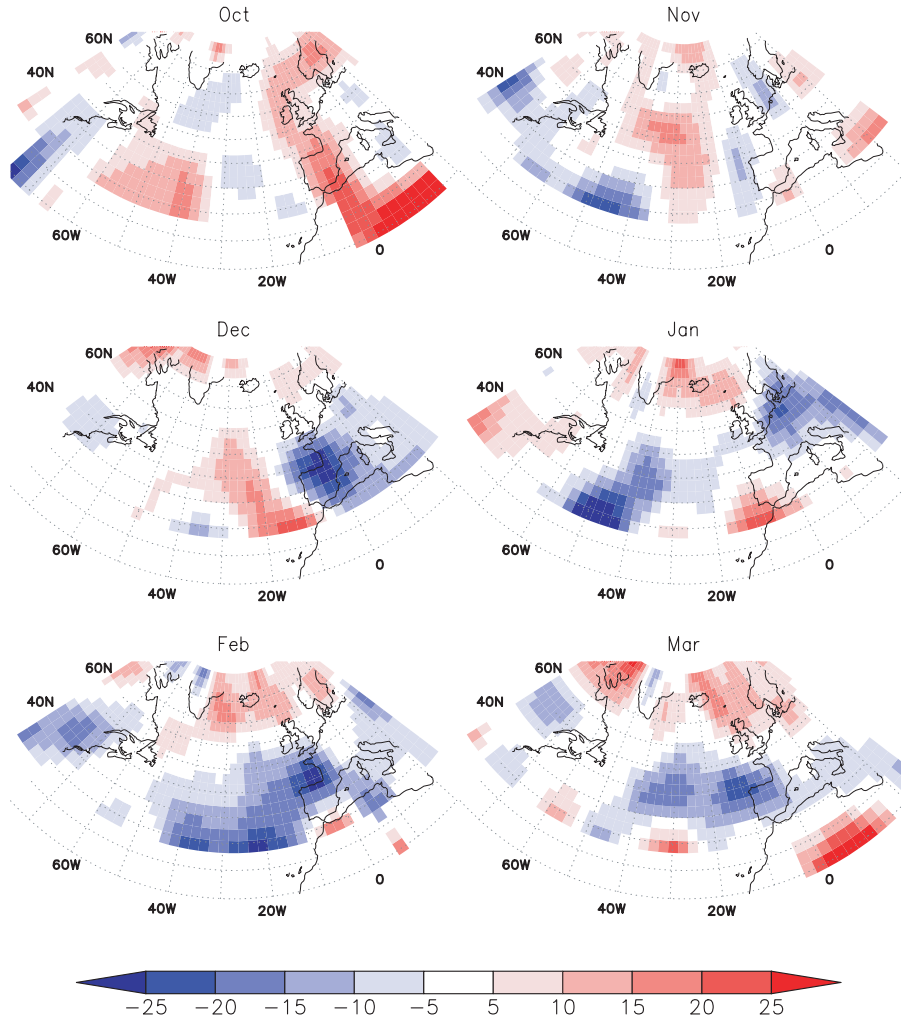
Figure 7. Decadal trends (% relative to the mean over the studied period) of the average number of cyclones detected in each winter month (October–March). Results are shown only for cells with the most significant trends. Statistics were computed for cell boxes with 9° longitude by 9° latitude for the period 1960–2000.

organized within latitudinal bands. The northern (southern) sector of the North Atlantic, between Greenland and Scandinavia (Azores and Mediterranean) presents an important increase (decrease) of both cyclonic activity (Fig. 7) and wind speed (Fig. 8).

The decline in cyclonic activity in February and March between Newfoundland and the Iberian Peninsula is particularly impressive. In fact, the negative trend extending from the Azores archipelago, in the mid-Atlantic Ocean, to the west of Iberia is significant at least at

10%. The average decline in cyclone count per decade reaches values over 20% over the Azores and north of Iberia (February) and at the northwest of Iberia (March). Such values per decade represent a decrease of over 60% of cyclonic centers between the first and last decades on record (relative to the first decade). In contrast, the area between Scotland, Iceland, and Scandinavia reveals a strong increase (significant at 10%) during February and March of more than 15% per decade at its maximum (relative to the period's average), which
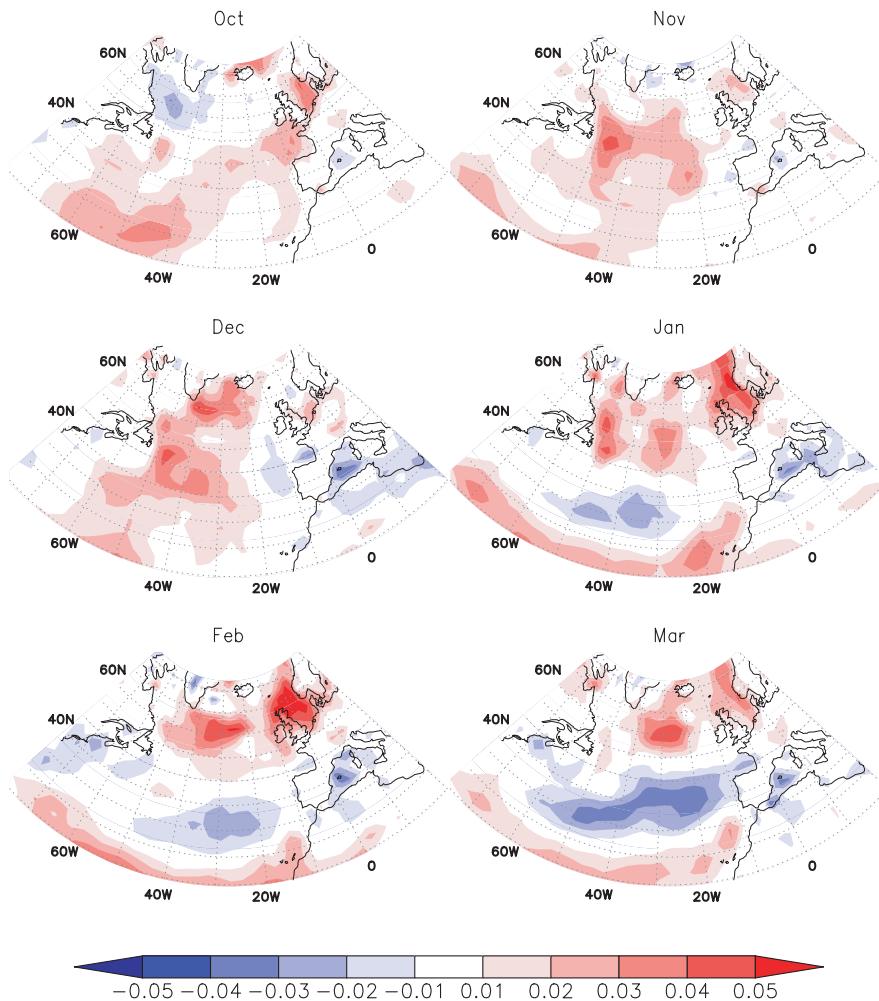
Figure 8. Trends of 10-m wind speed (m/s/year) detected in each winter month (October–March) for the period 1960–2000.

corresponds to an increment of roughly 50% between the first and last decades.

European Precipitation

Significant changes in the frequency of Atlantic cyclones aiming for Europe will inevitably lead to significant changes in the precipitation regime of the adjacent continental areas, including northern Africa, the Mediterranean basin, and central and northern Europe. Previous works have dealt with this link between long-term tendencies of cyclonic activity and precipitation, particularly for winter months, e.g. Ref. 5. This link has

been well documented for the month of March, which is characterized by a steep decline (increase) in precipitation in southwestern (northern) Europe and associated cyclonic activity.[10,57] Here we extend this analysis to the remaining winter months, using the high resolution precipitation data set from the CRU to compute the monthly precipitation trends for the extended winter season between 1960 and 2000 (Fig. 9). We have highlighted those regions that are characterized by statistically significant trends at less than 10% significance level (after applying a Mann–Kendall test). Despite some patchiness, it is possible to assert the following conclusions:
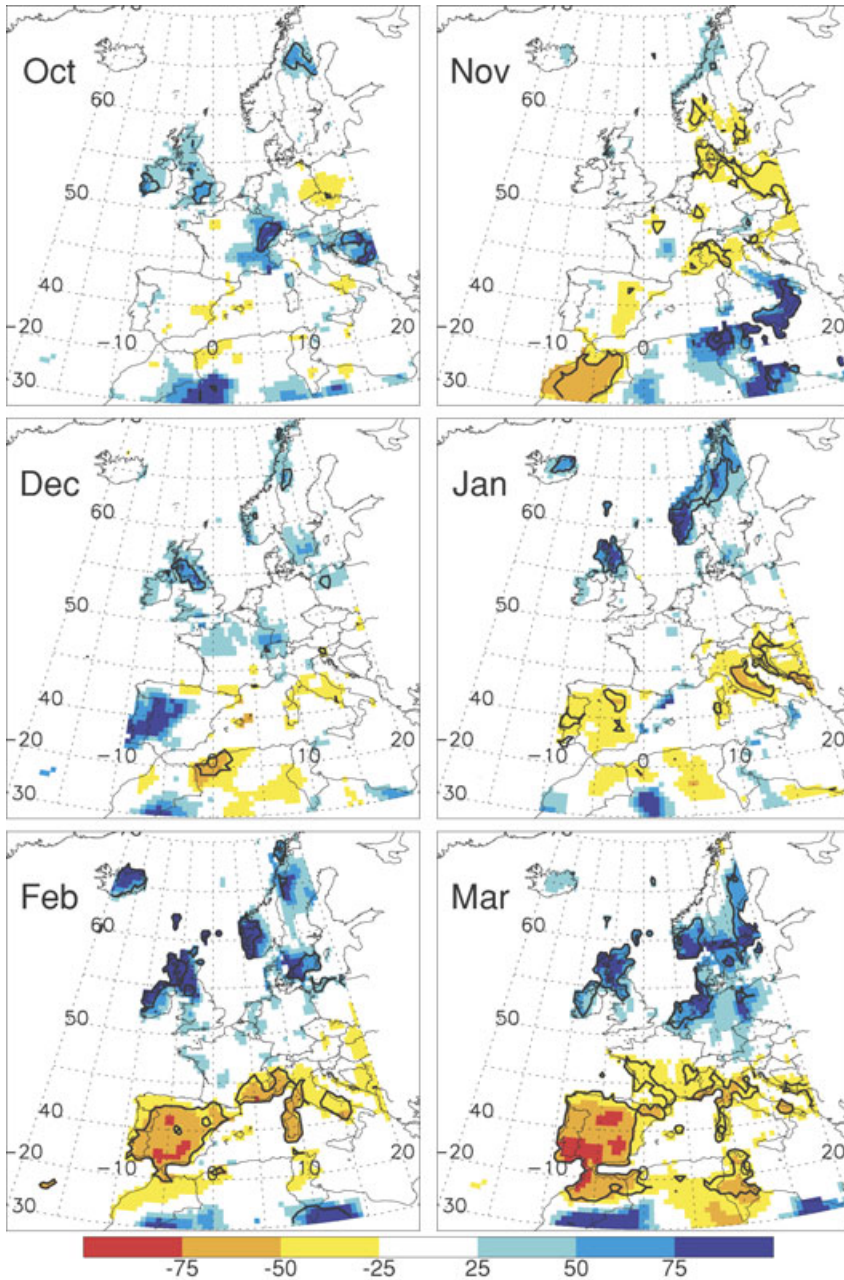
Figure 9. Relative change in monthly precipitation (%) over Europe for the period 1960–2000, computed from the Climatic Research Unit (CRU) monthly precipitation data set by applying a linear model. The black solid lines highlight those regions with statistically significant trends at less than 10%, obtained through a Mann–Kendall test.

a) Overall, there are more areas presenting a statistically significant decrease in precipitation than those characterized by an increment. This is particularly evident for southern Europe between January and March,

although a large region over the northeast of Africa in November also shows significant decreases.

b) There is a clear symmetrical division between northern and southern Europe in

terms of precipitation trends, particularly so during January–March. In fact, southern Europe is strongly affected by important decreases in precipitation from January to March in contrast to the significant increases over northern European countries during these months.

c) The northern European area, in particular the U.K. and Scandinavia, presents significant increments in precipitation throughout most of the considered months (with the exception of November).

For the purpose of performing an analysis of storm track activity and associated impact on precipitation, it is important to keep in mind that the algorithm used to track storms identifies and follows cyclone *centers* and the anomalies described in Figure 7 correspond to densities of storm centers. Therefore, the associated impact on precipitation extends to the south of regions where changes in cyclonic activity are verified and accompany the main fronts associated with the synoptic systems tracked by the algorithm. Despite this consideration, the combined analysis of cyclone trends and large-scale precipitation over land gives a very useful and complementary perspective to the main issue under analysis in this work. Both Figures 7 and 9 effectively show that changes in the location of cyclones are highly related to contemporaneous changes in precipitation averaged over the adjacent areas. This is clearly evident for northern Europe throughout all of the wet season months. Statistically significant cyclone positive trends over the region between Greenland and Scandinavia are reflected in significant increased precipitation over land. Moreover, the strong decreasing cyclone activity over the Atlantic area during February and March had a notable impact on Mediterranean precipitation, particularly over Iberia where winter core average precipitation is mainly related to low-pressure transient systems with an Atlantic origin.[10,65] Thus, it is possible to assert that the northern–southern European pattern of precipitation trends during the 1960–2000

core winter months was mainly related to similar changes in cyclone activity along the NAE sector.

Significant Wave Height in the Atlantic

A time linear regression was applied to the two 1970–2000 SWH data sets (original and corrected); however, in this paper we only present the results obtained with the corrected version (Fig. 10). A Mann–Kendall significance test was applied to the SWH trends presented in Figure 10. Most trends that are larger than 2 cm per year (either positive or negative) are statistically significant at the 5% level. We note that in the North Atlantic region, trends computed for the original ERA-40 data set show larger significance values (lower Mann–Kendall test values) than the corrected trends from October to December, a period dominated by positive trends in this region.

Once again monthly trends present a marked difference between the earlier and later winter period. Between October and December the vast majority of the North Atlantic Ocean is characterized by positive trends with maximum values (<2.5 cm/year) occurring between the U.K. and Iberia (October), west of Iberia (November), and close to the Azores in the mid-Atlantic (December). During the following 3 months (January to March) a different pattern emerges with positive values being found in the most northerly latitudes and negative trends positioned to the south at the Iberian Peninsula latitude and in the Mediterranean basin. Maximum positive trends (>3 cm/year) take place close to Greenland (January) and between the U.K. and Iceland in the following 2 months. February is the month that presents the largest negative trends south of lat 50°N, between -2 and -3 cm/year in the corrected data set. The SWH also increases in February with values of up to 5 cm/year just north of Scotland.

We would like to emphasize the agreement between the SWH trend results and those
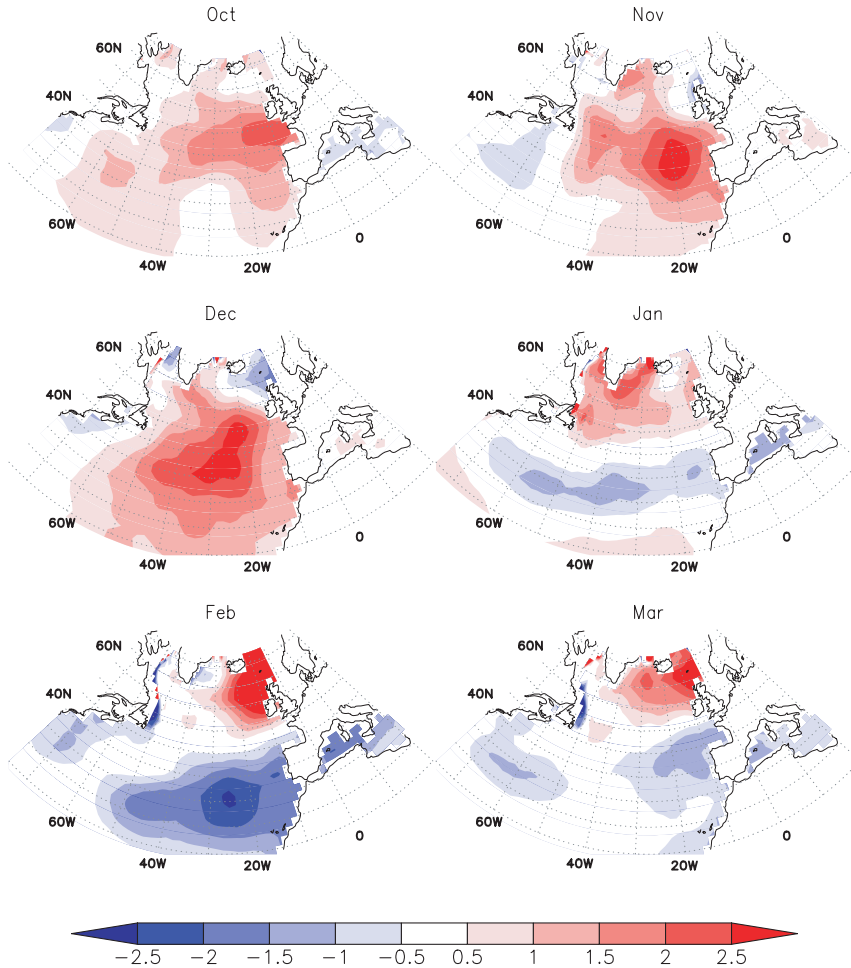
Figure 10. Monthly significant wave height trends (cm/year) for the period 1970–2000. Data correspond to the corrected ERA-40 values.

obtained for wind (Fig. 8) and cyclones (Fig. 7). In fact, throughout the extended winter months, regions with positive (negative) wind magnitude trends almost always have positive (negative) SWH trends. Nevertheless, in some cases this correspondence does not occur. For instance, in November and December the wind magnitude shows a weak negative trend to the northwest of the Iberian Peninsula that is not mirrored by the wave height trends. For the core winter months (January to March) the correspondence is well marked and both cyclone, wind magnitude, and SWHs show a distinct dipole of negative trends at lower latitudes and positive trends at higher latitudes in the North Atlantic. However, whereas February is

the month with the largest wave height trends in the Atlantic, March is the month for the highest wind magnitude. We emphasize that the analyzed periods are not the same for the variables, with the wind period (1960–2000) being longer than the wave height period (1970–2000).

Large-scale Atmospheric Patterns

Impact on Wind and Cyclones

We have computed the monthly/seasonal spatial correlation pattern for the wind speed and the corresponding monthly/seasonal indices of major atmospheric circulation patterns
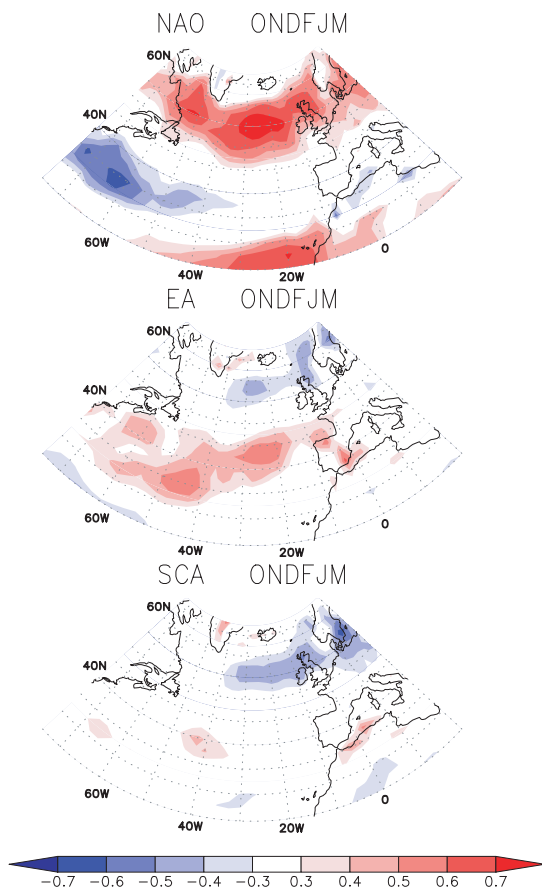
Figure 11. Correlation between winter (October–March) values of wind speed and the corresponding winter (top) NAO, (middle) EA, and (bottom) SCAND indices for the period 1960–2000.

that affect the NAE area. A similar procedure was applied to the corrected SWH fields for the entire North Atlantic basin and the indices of those same atmospheric circulation patterns. Results obtained at the seasonal scale can be seen in Figures 9 and 11 (SWH and wind, respectively). We have restricted the presentation of results to the aggregated winter (October–March) patterns for the sake of space and also because the corresponding individual monthly patterns are very similar (figures not shown). To facilitate the analysis of these two figures, SWH (wind) correlation values above 0.4 (0.3) and below −0.4 (−0.3) are statistically significant at the 5% significance level.

The highest correlation values are found (for both variables) with the NAO index, particularly over northern latitudes. The wind speed patterns present three latitudinal bands with different correlation signals, with the positive bands stretching between Newfoundland and Scandinavia in the north and a subtropical band reaching the West African coast (Fig. 11, top). The mid-latitude band located in between shows a negative trend pattern, particularly on the western side of the Atlantic and some scattered areas in the Mediterranean. The corresponding NAO correlation pattern for the SWH presents an area with very high positive correlation values in the north between Greenland and the U.K. ($R > 0.7$), while the central sector of the North Atlantic shows negative values that are slightly smaller in magnitude ($R \leq 0.6$). Negative values are also found within the Mediterranean Sea (Fig. 12, top).

Correlations between wind and the EA index are less strong than those found with the NAO index, with values never surpassing 0.6 (Fig. 11, middle). The same assessment applies to the EA–SWH pattern with the highest values ranging from slightly below −0.5 to just above +0.7 (Fig. 12, middle). However, the EA–SWH correlation presents a much more coherent positive spatial configuration, unlike the typical dipole observed in the NAO-SWH pattern. A relatively small pattern of negative (positive) correlation values is found for both variables with maxima located between Iceland and the U.K. (Mediterranean Sea).

It is worth mentioning that the location of maximum correlation values for these two indices (NAO and EA) and the SWH fields is usually east of the corresponding maximum values obtained for the wind pattern. This result is to be expected because the magnitude of SWH depends not only on the local wind speed but also on the magnitude of the swell associated with distant storms,[13,14] which contribute to the upward or downward pile effect close to the European and African coasts. The link between the patterns obtained in these two figures now becomes obvious because the
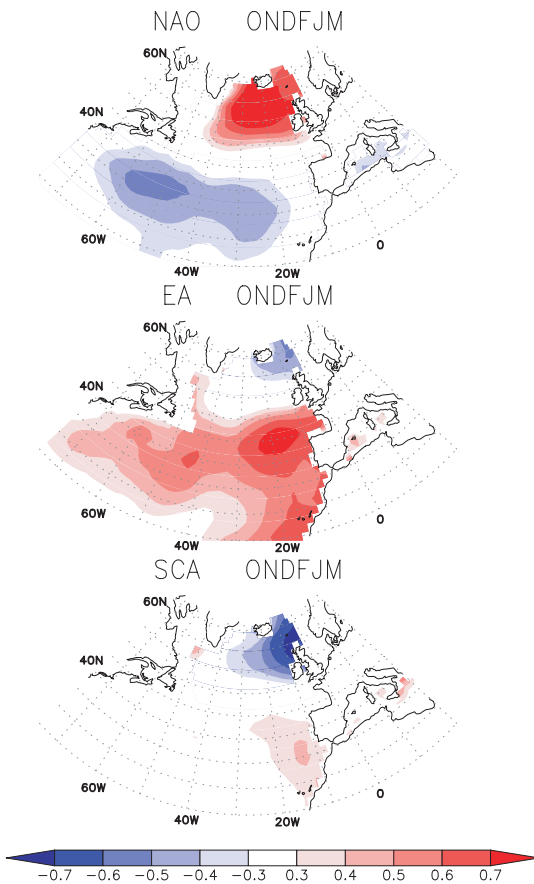
Figure 12. Correlation between winter (October–March) values of significant wave height (corrected values) and the corresponding winter (top) NAO, (middle) EA, and (bottom) SCAND indices for the period 1970–2000.

surface winds and associated cyclones at mid- to high-latitudes blow with mainly a westerly component.[11] This is not the case at subtropical latitudes where the easterly trade winds prevail,[66] impeding the appearance of a third region with high values of correlation with the NAO index.

The correlation pattern between the wind and the SCAND index is relatively weak and almost confined to the northeastern sector of the Atlantic, between Greenland and Scandinavia (Fig. 11, bottom). Similarly, the highest correlation values observed between SWH–SCAND are dominated by a north–south negative/positive dipole (Fig. 12, bottom). Positive correlations are relatively high close to Iberia and the North African coast, while negative val-

ues can be mostly observed north of the British Islands and also close to Newfoundland (for the wind). It should be remembered that the SCAND circulation pattern is the most continental teleconnection pattern used in this work (Fig. 5) and its impact in both the wind and SWH fields is expected to be confined to the ocean sector close to Europe.

Impact on European Precipitation

We have also computed the monthly/seasonal spatial correlation pattern between European precipitation (high resolution CRU data set) and the corresponding monthly/seasonal indices of the three atmospheric circulation patterns considered. However, in this section we present the entire set of results obtained for each winter month. This approach was necessary to take into account the large spatial and temporal variability that characterizes the precipitation field over Europe. We have only shown those grid boxes characterized by correlation values statistically significant at least at the 10% significance level (Figs. 10–12). No precipitation information is available from the oceans as our data set is constructed with precipitation values from rain gauges. In agreement with the work developed by other authors, our data show that other modes besides NAO play an important role in shaping European precipitation variability, e.g., Refs. 61–63, 67, 68. While the NAO pattern is one of the three leading causes of variability in the Northern Hemisphere SLP, at the monthly scale, throughout the whole year (except in September), the remaining modes used are less important. As a consequence, some of these modes have a smaller amplitude and regional characteristics during part of the year,[29] therefore the intensity of their impacts is slightly reduced compared with the NAO pattern.

The typical winter NAO–precipitation pattern shown in Figure 13 is in agreement with the results obtained recently by many authors, e.g., Refs. 5, 35, 36, 40. The most prominent correlations can be observed between
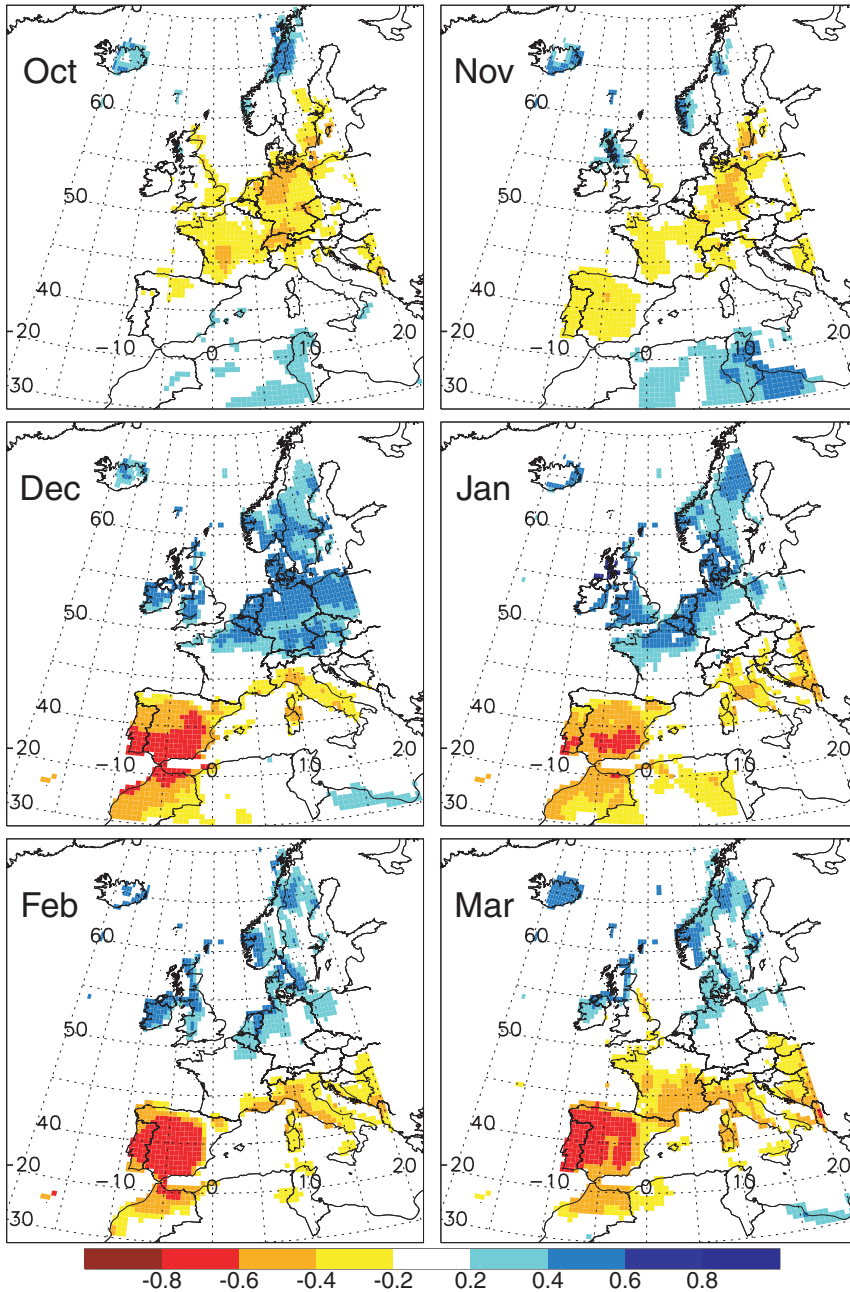
Figure 13. Correlation values between monthly European precipitation (CRU data set) and the corresponding monthly value of NAO index for the period 1960–2000.

December and March (Fig. 13), with large negative values over Iberia ($r \leq 0.7$), northern Africa, and the central Mediterranean; positive values dominate over northern Europe, albeit with a smaller magnitude ($r < 0.6$). However, a different pattern emerges in October and November with weak but significant negative correlation values for most of Europe between Iberia and southern Scandinavia; positive values remain confined to small scattered patches of the U.K., Scandinavia, and most of northern Africa (Fig. 13).
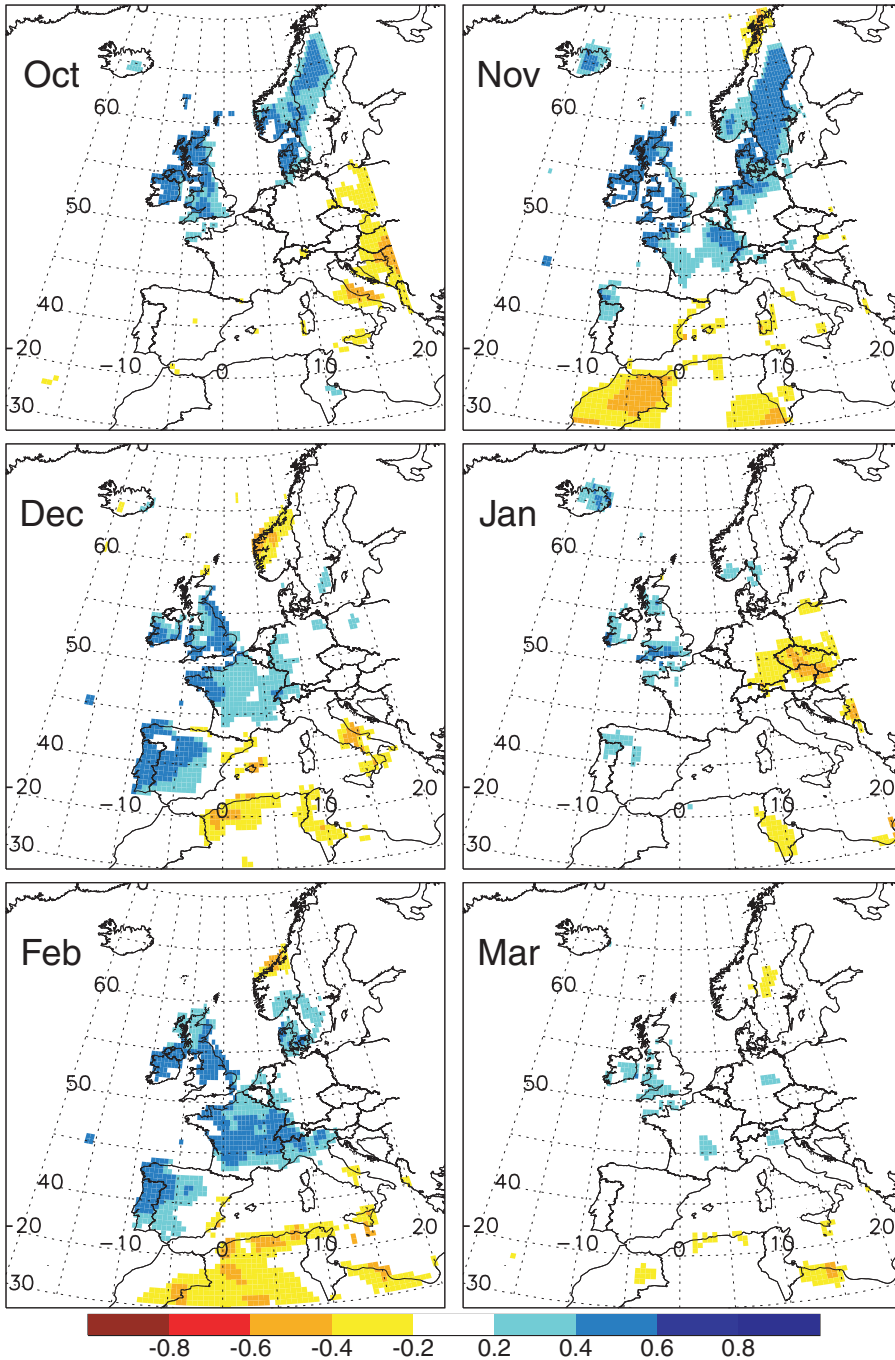
Figure 14. Correlation values between monthly European precipitation (CRU data set) and the corresponding monthly value of EA index for the period 1960–2000.

Recent works have shown that the EA pattern represents a significant contribution to precipitation over northern Iberia[69,70] as well as parts of the eastern Mediterranean areas.[4,61,67]

The EA–precipitation correlation pattern that we show is less pronounced (lower values) and less consistent throughout the winter months when compared with the NAO–precipitation
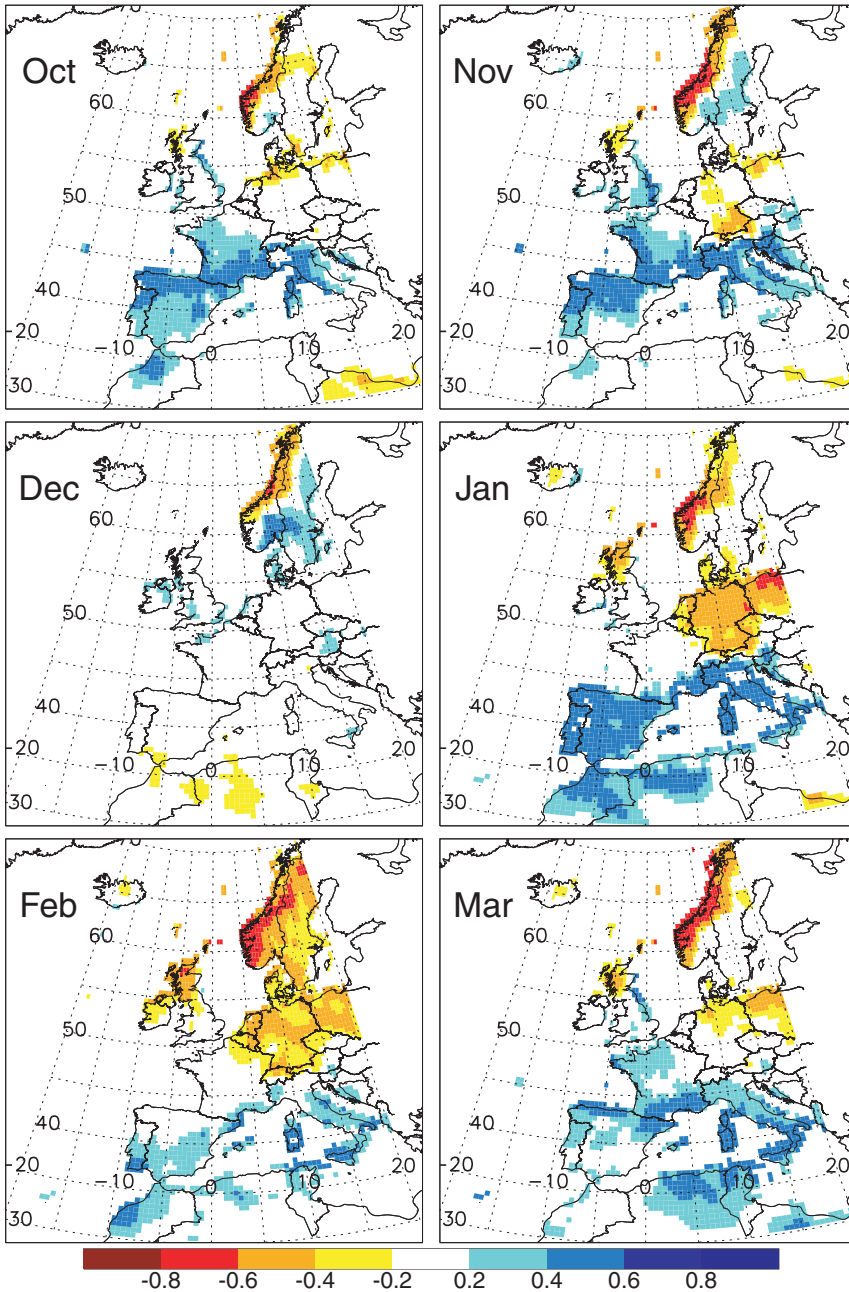
Figure 15. Correlation values between monthly European precipitation (CRU data set) and the corresponding monthly value of SCAND index for the period 1960–2000.

pattern, being almost negligible in March (Fig. 14). Nevertheless, significant positive values dominate the western European facade with higher values ($r > 0.5$) being found from the U.K. to Scandinavia in October and November and between the U.K. and Iberia be-

tween December and February. Negative correlation values prevail in northern Africa and the central Mediterranean, with scattered secondary centers being observed in eastern Europe (October and December) and Norway (November and December).

Interestingly, results obtained with the corresponding SCAND–precipitation correlation monthly patterns present higher correlation values than those obtained with the EA pattern (Fig. 15). These results are in agreement with those of previous authors that have shown that the SCAND pattern is associated with important precipitation anomalies in both western and eastern Mediterranean regions.[40,61,71] With the exception of December, all the remaining months are characterized by significant positive correlation values covering the Mediterranean basin. On the contrary, the western half of the Scandinavian peninsula (Norway) presents a persistent, large, negative value, lower then −0.6 over some grid boxes. The region between Germany and Poland is also characterized by negative values, particularly between January and March (Fig. 15).

Conclusions

The first part of this study presented an integrated analysis of the frequency of cyclones and near surface (10-m) wind speed over the NAE sector using the ERA-40 reanalysis data for the extended winter and covering the 1960–2000 period. A comprehensive comparison between these trends and those of SWH [computed by the KNMI[13] from the ERA-40 reanalysis (1970–2000)] and the CRU land precipitation data set[45] was then made. Previous papers have evaluated the impact of both cyclones and wind patterns on either SWH, e.g., Ref. 14, or precipitation, e.g., Ref. 5. However, to the best of our knowledge, none of these previous works have provided an all-encompassing impact analysis of the weather systems upon the ocean waves (SWH) and the climate of adjacent continental areas (precipitation) as we have presented here.

Our results revealed large changes in cyclone frequencies for the last four decades, particularly during the late winter months when significant decreases were found between the Azores archipelago and the western Mediterranean. In contrast, the Artic sector of the northern

Atlantic (between Greenland and Scandinavia) suffered a significant increase in cyclones. In February and March the density of cyclones declined at an average rate of 20% per decade in some regions, corresponding to more than a 60% decrease between the first and last decades on record. On the other hand, the northern NAE region was marked by increments of up to 50% in January–March cyclone frequencies between the first and last decades during the same period. These results indicate that the opposite cyclone trends observed in southern and northern Europe are not restricted to March as previously hypothesized,[10] but are more widespread in time. Trends for wind speed obtained in this work (reaching up to 5 cm/year) were shown to be in good agreement with the trends for corresponding cyclone frequency, with a close match being found between regions affected by negative and positive trends for both variables.

Using the CRU high resolution land precipitation data set, it was possible to confirm the link between precipitation trends and cyclone frequencies for the extended winter season. It must be stressed that such an association is harder to establish for a number of reasons. In particular, the impact on precipitation extends to the south of each main minimum of pressure tracked by the algorithm used here. Nevertheless, there is a spatial coherence between both trend patterns obtained in this work, with decreases (increases) in precipitation appearing close to areas characterized by negative (positive) cyclone frequency trends. Precipitation trends over Europe during January–March reveal a contrasting latitudinal band structure between northern and southern Europe, with southern (northern) Europe presenting important decreases (increases) in precipitation.

The computation of SWH trends for the North Atlantic revealed very well-marked regions with variations that were almost always coincident with the cyclone and wind speed trend patterns. In particular, the early winter months are characterized by a wide region of positive wave height trends in the North Atlantic that is more widespread spatially than

in the cyclone and wind speed case. As for cyclone frequencies and wind speed, a dipole of positive/negative SWH trends for January–March was also detected between the Greenland–Scandinavian latitudes and south of lat 50°N, with the largest trends occurring in February (−3 cm/year and +5 cm/year).

In the final part of this study we focused on the connection between the previous changes and the preferred phases of major large-scale atmospheric circulation modes or teleconnections (NAO, EA, and SCAND). Correlations between these indices and both wind speed and SWH were presented for the aggregated winter months October–March. Absolute correlation values higher than 0.7 with the NAO and the EA patterns were obtained over certain sectors of the North Atlantic basin. As expected, NAO was found to be positively correlated with wind speed and SWH at high to mid-latitudes and negatively correlated at mid- to low latitudes. On the other hand, negative correlation values were computed between EA and wind speed and SWH for high latitudes, whereas an extensive area of positive correlations was obtained for the mid- to low latitudes. We found that maximum correlation values for SWH with the NAO and EA indices were generally located to the east of maximum correlation values for the wind. Minor but still significant correlation values were also obtained for SCAND, particularly at high latitudes close to the NAE area where negative correlations lower than −0.6 were computed.

The impact of the three large-scale circulation modes on European precipitation was evaluated at the monthly scale, in order to address the large spatial and temporal variability that is a trademark of the precipitation field. The signature on precipitation of the three corresponding modes analyzed is clearly noticeable for the whole European continent. Although the NAO is the most prominent teleconnection for the entire North Atlantic region and, consequently, explains the highest fraction of precipitation variability over Europe, the EA and SCAND patterns also present notable in-

fluences on European rainfall. Naturally, the intensity and the aspect of their spatial impact in the precipitation patterns differ from one to another. While the NAO signature on precipitation is reflected in the consistent and well-known positive (Northern Europe) and negative (Iberia) European precipitation dipole from December to March, the influences of EA and SCAND present a higher intramonthly intensity and spatial variability. Nevertheless, the SCAND pattern explains a higher fraction of precipitation variability compared with the EA mode. This is mainly reflected in the larger negative correlated area covering the whole Mediterranean basin throughout the winter season, while the EA influence is reduced to central and northern Europe for some winter months. Thus, a comprehensive analysis of several large-scale modes is a key factor for assessing the precipitation–circulation relation and providing the physical mechanisms responsible for the large winter precipitation trends found in Europe.

Finally, we would like to address the possible impact of anthropogenic climate change in cyclonic activity caused by increased greenhouse gases in the atmosphere. The current generation of global circulation models (GCMs) has shown a reasonable capacity to reproduce the spatial pattern of cyclones for current climate.[23,72] According to these authors[23,72] we can expect significant changes in the winter mid-tropospheric storm tracks independently from the emissions scenario adopted, with particularly large activity increases downstream of the Atlantic storm track over western Europe.[23] However, the magnitude of this signal is largely dependent on the imposed change in forcing. A common feature of all investigated GCMs is a reduced track density over central Europe under climate change conditions if all systems are considered.[72] If only extreme cyclones are considered, increased cyclone activity for western parts of central Europe prevails. With respect to extreme wind speeds, significant positive changes in intensity and frequency are obtained over certain areas of Europe.[72]

Conflicts of Interest

The authors declare no conflicts of interest.

References

1. Trenberth, K.E., P.D. Jones, P. Ambenje, *et al*. 2007. Observations: surface and atmospheric climate change. In *Climate Change 2007: The Physical Science Basis. Contribution of Working Group I to the Fourth Assessment Report of the Intergovernmental Panel on Climate Change*. S. Solomon, D. Qin, M. Manning, *et al*., Eds.: Cambridge University Press. Cambridge, United Kingdom and New York, NY, USA.

2. Jones, P.D. & A. Moberg. 2003. Hemispheric and large-scale surface air temperature variations: an extensive revision and an update to 2001. *J. Clim.* **16:** 206–223.

3. Delitala, A.M.S., D. Cesari, P.A. Chessa & M.N. Ward. 2000. Precipitation over Sardinia (Italy) during the 1946–1993 rainy season and associated large-scales climate variations. *Int. J. Climatol.* **20:** 519–541.

4. Xoplaki, E., J.F. González-Rouco, J. Luterbacher & H. Wanner. 2004. Wet season Mediterranean precipitation variability: influence of large-scale dynamics. *Clim. Dyn.* **23:** 63–78.

5. Trigo, I.F. 2006. Climatology and interannual variability of storm-tracks in the Euro-Atlantic sector: a comparison between ERA-40 and NCEP/NCAR reanalyses. *Clim. Dyn.* DOI 10.1007/s00382-005-0065-9.

6. Schönwiese, C.D. 1993. *Klimatrend-Atlas Europa 1891–1990 (Atlas of climate trends for Europe 1891–1990)*. Verlag, Zentrum für Umweltforschung. Frankfurt. 218 pp.

7. Hoppe, H. & G. Kiely. 1999. Precipitation over Ireland—Observed change since 1940. *Phys. Chem. Earth.* **24:** 91–96.

8. Kiely, G., J.D. Albertson & M. Parlange. 1998. Recent trends in diurnal variation of precipitation at Valentia on the West coast of Ireland. *J. Hydrol.* **207:** 270–279.

9. Klein, A.M.G. *et al*. 2002. Daily dataset of 20th-century surface air temperature and precipitation series for the European Climate Assessment. *Int. J. Climatol.* **22:** 1441–1453.

10. Paredes, D., R.M. Trigo, R. Garcia-Herrera & I.F. Trigo. 2006. Understanding precipitation changes in Iberia in early Spring: weather typing and storm-tracking approaches. *J. Hydrometeor.* **7:** 101–113.

11. Gulev, S.K. & V. Grigorieva. 2004. Last century changes in ocean wind wave height from global visual wave data. *Geophys. Res. Lett.* **31:** L24302, doi: 10.1029/2004GL021040.

12. Caires, S. & A. Sterl. 2005. 100-year return value estimates for ocean wind speed and significant wave height from the ERA-40 data. *J. Clim.* **18:** 1032–1048.

13. Sterl, A. & S. Caires. 2005. Climatology, variability and extrema of ocean waves: the web-based KNMI/ERA-40 Wave Atlas. *Int. J. Climatol.* **25:** 963–977.

14. Wang, X.L. & V.R. Swail. 2002. Trends of Atlantic wave extremes as simulated in a 40-yr wave hindcast using kinematically reanalyzed wind fields. *J. Clim.* **15:** 1020–1035.

15. Ferranti, L. & P. Viterbo. 2006. The European summer of 2003: sensitivity to soil water initial conditions. *J. Clim.* **19:** 3659–3680.

16. Gulev, S.K., O. Zolina & S. Grigoriev. 2001. Extratropical cyclone variability in the Northern Hemisphere winter from the NCEP/NCAR reanalysis data. *Clim. Dyn.* **17:** 795–809.

17. Wang, X.L., V.R. Swail & F.W. Zwiers. 2006. Climatology and changes of extratropical storm tracks and cyclone activity: comparison of ERA-40 with NCEP/NCAR Reanalysis for 1958–2001. *J. Clim.* **19:** 3145–3166.

18. Raible, C.C., P. Della-Marta, C. Schwierz, *et al*. 2008. Northern Hemisphere extratropical cyclones: a comparison of detection and tracking methods and different reanalyses. *Mon. Wea. Rev.* **136:** 880–897.

19. Alexander, L.V., S.F.B. Tett & T. Jonsson. 2005. Recent observed changes in severe storms over the United Kingdom and Iceland. *Geophys. Res. Lett.* **32:** L13704.

20. Alexandersson, H., H. Tuomenvirta, T. Schmith & K. Iden. 2000. Trends of storms in NW Europe from an updated pressure data set. *Clim. Res.* **14:** 71–73.

21. Bärring, L. & H. von Storch. 2004. Scandinavian storminess since about 1800. *Geophys. Res. Lett.* **31:** L20202, doi 10.1029/2004GL020441.

22. Andrade, C., R.M. Trigo, M.C. Freitas, *et al.* 2008. Comparing historic records of storm frequency and the North Atlantic Oscillation (NAO) chronology for the Azores region. *The Holocene* **18:** 745–754, DOI 10.1177/0959683608091794.

23. Pinto, J.G., E.L. Fröhlich, G.C. Leckebusch & U. Ulbrich. 2007. Changes in storm loss potentials over Europe under modified climate conditions in an ensemble of simulations of ECHAM5/MPI-OM1. *Nat. Hazards Earth Syst. Sci.* **7:** 165–175.

24. Miller, C. 2003. A once in 50-year wind speed map for europe derived from mean sea level pressure measurements. *J. Wind Engng. Ind. Aerodyn.* **91:** 1813–1826.

25. Pryor, S.C., R.J. Bathelmie & J.T. Schoof. 2006. Inter-annual variability of wind indices across Europe. *Wind Energy* **9:** 27–38.

26. Walter, A., K. Keuler, D. Jacob, *et al.* 2006. A high resolution reference data set of german wind velocity 1951–2001 and comparison with regional climate model results. *Meteorol. Zeitschrift* **15:** 585–596.

27. Mendes, D., E. Souza, I. Trigo & P.M.A. Miranda. 2007. On precursors of south American cyclogenesis. *Tellus A.* **59:** 114–121.

28. Trigo, I.F., G.R. Bigg & T.D. Davies. 2002. Climatology of cyclogenesis mechanisms in the Mediterranean. *Mon. Weather Rev.* **130:** 549–569.

29. Barnston, A.G. & R.E. Livezey. 1987. Classification, seasonality, and persistence of low-frequency atmospheric circulation patterns. *Mon. Wea. Rev.* **115:** 1083–1126.

30. Wallace, J.M. & D.S. Gutzler. 1981. Teleconnections in the geopotential height field during the Northern Hemisphere winter. *Mon. Wea. Rev.* **109:** 784–812.

31. Yarnal, B. 1993. *Synoptic Climatology in Environmental Analysis. A Primer, Studies in Climatology Series*. Belhaven Press. London.

32. Rex, D.F. 1950. Blocking action in the middle troposphere and its effect upon regional climate. Part I: an aerological study of blocking action. *Tellus* **2:** 196–211.

33. Rex, D.F. 1950. Blocking action in the middle troposphere and its effect upon regional climate. Part II: the climatology of blocking action. *Tellus* **2:** 275–301.

34. Rex, D.F. 1951. The effect of Atlantic blocking action upon European climate. *Tellus* **3:** 1–16.

35. Hurrell, J.W. 1995. Decadal trends in the north Atlantic oscillation: regional temperatures and precipitation. *Science* **269:** 676–679.

36. Hurrell, J.W., Y. Kushnir, G. Ottersen & M. Visbeck. 2003. The North Atlantic Oscillation: climate significance and environmental impact. *Geophysical Monograph Series*, **134:** 279 pp.

37. Jones, P.D., M. Hulme & K.R. Briffa. 1993. A comparison of Lamb circulation types with an objective classification scheme. *Int. J. Climatol.* **13:** 655–663.

38. Lamb, H. 1972. British Isles weather types and a register of daily sequence of circulation patterns, 1861–1971. *Geophysical Memoir* **116**, HMSO, London, 85 pp.

39. Hess, P. & H. Brezowski. 1977. Katalog der Grosswetterlagen Europas (1881–1976) Berichte des Deutschen Wetterdienstes 113(15). Selbstverlag des Deutshen Wetterdienstes, Offenbach am Main.

40. Corte-Real, J., X. Zhang & X. Wang. 1995. Large-scale circulation regimes and surface climatic anomalies over the Mediterranean. *Int. J. Climatol.* **15:** 1135–1150.

41. Dünkeloh, A. & J. Jacobeit. 2003. Circulation dynamics of Mediterranean precipitation variability 1948–1998. *Int. J. Climatol.* **23:** 1843–1866.

42. Xoplaki, E., J.F. González-Rouco, J. Luterbacher & H. Wanner. 2003. Mediterranean summer air temperature variability and its connection to the large-scale atmospheric circulation and SSTs. *Clim. Dyn.* **20:** 723–739.

43. Trigo, R.M. & J.P. Palutikof. 2001. Precipitation scenarios over Iberia: a comparison between direct GCM output and different downscaling techniques. *J. Clim.* **14:** 4422–4446.

44. New, M.G., Hulme M. & Jones P.D. 1999. Representing twentieth-century space-time climate variability. Part I: development of a 1961–90 mean monthly terrestrial climatology. *J Clim.* **12:** 829–856.

45. New, M.G., Hulme M. & Jones P.D. 2000. Representing twentieth-century space-time climate variability. Part II: development of a 1901–95 monthly grids of terrestrial surface climate. *J Clim.* **13:** 2217–2238.

46. Uppala, S.M. *et al.* 2005. The ERA-40 Reanalysis. *Q. J. Roy. Meteor. Soc.* **131:** 2961–3012, doi: 10.1256/qj.04.176.

47. Blender, R., K. Fraedrich & F. Lunkeit. 1997. Identification of cyclone track regimes in North Atlantic. *Q. J. R. Meteorol. Soc.* **123:** 727–741.

48. Hodges, K.I. 1994. A general method for tracking analysis and its application to meteorological data. *Mon. Wea. Rev.* **122:** 2573–2586.

49. Murray, R.J. & I. Simmonds. 1991. A numerical scheme for tracking cyclone centres from digital data. Part 1: development and operation of the scheme. *Aust. Met. Mag.* **39:** 155–166.

50. Serreze, M.C., F. Carse, R.G. Barry & J.C. Rogers. 1997. Icelandic low cyclone activity: climatological

features, linkages with the NAO, and relationships with recent changes in the northern hemisphere circulation. *J. Clim.* **10:** 453–464.

51. Trigo, I.F., T.D. Davies & G.R. Bigg. 1999. Objective climatology of cyclones in the Mediterranean Region. *J. Clim.* **12:** 1685–1696.

52. Gray, S. L. & H. F. Dacre. 2006. Classifying dynamical forcing mechanisms using a climatology of extratropical cyclones. *Q. J. R. Met. Soc.* **132:** 1119–1137.

53. Wernli, H. & C. Schwierz. 2006. Surface cyclones in the ERA-40 data set (1958–2001). Part I: novel identification method and global climatology. *J. Atmos. Sci.* **63:** 2486–2507.

54. Hoskins, B.J. & K. I. Hodges. 2002. New perspectives on the northern hemisphere winter storm tracks. *J. Atmos. Sci.* **59:** 1041–1061.

55. Pinto, J. G., T. Spangehl, U. Ulbrich & P. Speth. 2005. Sensitivities of a cyclone detection and tracking algorithm: individual tracks and climatology. *Meteorol. Zeitschrift* **14:** 823–838.

56. Trigo, R.M., I.F. Trigo, C.C. DaCamara & T.J. Osborn. 2004. Climate impact of the European winter blocking episodes from the NCEP/NCAR Reanalyses. *Clim. Dyn.* **23:** 17–28.

57. Garcia-Herrera, R., D. Paredes, R.M. Trigo, *et al.* 2007. The outstanding 2004–2005 drought in the Iberian Peninsula: associated atmospheric circulation. *J. Hydrometeor.* **8:** 483–498.

58. Caires, S. & A. Sterl. 2005. A new non-parametric method to correct model data: application to significant wave height from the ERA-40 reanalysis. *J. Atmos. Oceanic Tech.* **22:** 443–459.

59. Simmons, A.J. 2001. Development of the ERA-40 data assimilation system. In *Proc. of the ECMWF Workshop on Re-analysis*, ERA-40 Project Report Series (3, 11–30). 5–9 November, Reading.

60. Komen, G.J., L. Cavaleri, M. Donelan, *et al.* 1994. *Dynamics and Modelling of Ocean Waves.* Cambridge University Press. Cambridge.

61. Qian, B., J. Corte-Real & H. Xu. 2000. Is the North Atlantic Oscillation the most important atmospheric pattern for precipitation in Europe? *J. Geophys. Res.* **105:** 11901–11910.

62. Quadrelli, R., V. Pavan & F. Molteni. 2001. Wintertime variability of Mediterranean precipitation and its links with large-scale circulation anomalies. *Clim. Dyn.* **17:** 457–466.

63. Zorita, E., V. Kharin & H. von Storch. 1992. The atmospheric circulation and sea surface temperature in the North Atlantic in winter. Their interaction and relevance for Iberian rainfall. *J. Clim.* **5:** 1097–1108.

64. Trigo, R. *et al.* 2006. Relations between variability in the Mediterranean region and Mid-Latitude variability. In *The Mediterranean Climate: An Overview of the Main Characteristics and Issues.* P. Lionello, P. Malanotte-Rizzoli & R. Boscolo, Eds.: 179–226. Elsevier. Amsterdam.

65. Serrano, A., A.J. Garcia, V.L. Mateos, M.L. Cancillo & J. Garrido. 1999. Monthly modes of variation of precipitation over the Iberian Peninsula. *J. Clim.* **12:** 2894–2919.

66. Peixoto, J.P. & A.H. Oort. 1992. *Physics of Climate.* American Institute of Physics. New York.

67. Krichak, S.O., P. Kishcha & P. Alpert. 2002. Decadal trends of main Eurasian oscillations and the Eastern Mediterranean precipitation. *Theor. Appl. Climatol.* **72:** 209–220.

68. von Storch, H., E. Zorita & U. Cubasch. 1993. Downscaling of global climate change estimates to regional scales: An application to Iberian rainfall in wintertime. *J. Clim.* **6:** 1161–1171.

69. Rodriguez-Puebla, C., A.H. Encinas, S. Nieto & J. Garmendia. 1998. Spatial and temporal patterns of annual precipitation variability over the Iberian Peninsula. *Int. J. Climatol.* **18:** 299–316.

70. Sáenz, J., J. Zubillaga & C. Rodriguez-Puebla. 2001. Interannual variability of winter precipitation in northern Iberian Peninsula. *Int. J. Climatol.* **21:** 1503–1513.

71. Wibig, J. 1999. Precipitation in Europe in relation to circulation patterns at the 500 hPa level. *Int. J. Climatol.* **19:** 253–269.

72. Leckebusch, G.C., B. Koffi, U. Ulbrich, *et al.* 2006. Analysis of frequency and intensity of winter storm events in Europe on synoptic and regional scales from a multi-model perspective. *Clim. Res.* **31:** 59–74.